Targeting CD33+ Acute Myeloid Leukemia with GLK-33, a Lintuzumab-Auristatin Conjugate with a Wide Therapeutic Window

Satomaa, Tero

American Association for Cancer Research Inc.
2024-08-01

Satomaa, T, Pynnönen, H, Aitio, J, Hiltunen, J O, Pitkänen, V, Lähteenmäki, T, Kotiranta, T, Heiskanen, A, Hänninen, A-L, Niemelä, R, Helin, J, Kuusanmäki, H, Vänttinen, I, Rathod, R, Nieminen, A I, Yatkin, E, Heckman, C A, Kontro, M & Saarinen, J 2024, 'Targeting CD33+ Acute Myeloid Leukemia with GLK-33, a Lintuzumab-Auristatin Conjugate with a Wide Therapeutic Window', Molecular Cancer Therapeutics, vol. 23, no. 8, pp. 1073-1083. https://doi.org/10.1158/1535-71

http://hdl.handle.net/10138/590574
10.1158/1535-7163.MCT-23-0720

Targeting CD33+ acute myeloid leukemia with GLK-33, a lintuzumab-auristatin conjugate with a wide therapeutic window

Authors: Tero Satomaa[1], Henna Pynnönen[1], Olli Aitio[1], Jukka O. Hiltunen[1], Virve Pitkänen[1], Tuula Lähteenmäki[1], Titta Kotiranta[1], Annamari Heiskanen[1], Anna-Liisa Hänninen[1], Ritva Niemelä[1], Jari Helin[1], Heikki Kuusanmäki[2,3], Ida Vänttinen[2], Ramji Rathod[2], Anni I. Nieminen[2], Emrah Yatkin[4], Caroline A. Heckman[2], Mika Kontro[2,3,5], and Juhani Saarinen[1]

Affiliations:

[1]Glykos Finland Oy, Helsinki, Finland.

[2]Institute for Molecular Medicine Finland (FIMM), Helsinki Institute of Life Science (HiLIFE), University of Helsinki, Finland.

[3]Finnish Cancer Institute, Helsinki, Finland.

[4]Central Animal Laboratory, University of Turku, Finland.

[5]Department of Hematology, Helsinki University Hospital Comprehensive Cancer Center, Helsinki, Finland.

Running title: Targeting CD33+ acute myeloid leukemia with GLK-33

Keywords: CD33, AML, antibody-drug conjugate, auristatin, MMAU

Corresponding Authors: Tero Satomaa and Juhani Saarinen, Glykos Finland Oy, Phone: +358 9 3193 6340; E-mail: tero.satomaa@glykos.fi, juhani.saarinen@glykos.fi

Conflicts of Interest: The authors disclose potential conflicts of interest; please see the Acknowledgements page for details.

Text: <3800 words, **Abstract:** 197 words, **Figures:** 6, **References:** 59

Abstract

CD33 (Siglec-3) is a cell surface receptor expressed in approximately 90% of AML blasts, making it an attractive target for therapy of acute myeloid leukemia (AML). While previous CD33-targeting antibody-drug conjugates (ADCs) like gemtuzumab ozogamicin (GO, Mylotarg) have shown efficacy in AML treatment, they have suffered from toxicity and narrow therapeutic window. This study aimed to develop a novel ADC with improved tolerability and a wider therapeutic window. GLK-33 consists of the anti-CD33 antibody lintuzumab and eight mavg-MMAU auristatin linker-payloads per antibody. The experimental methods included testing in cell cultures, patient-derived samples, mouse xenograft models, and rat toxicology studies. GLK-33 exhibited remarkable efficacy in reducing cell viability within CD33-positive leukemia cell lines and primary AML samples. Notably, GLK-33 demonstrated anti-tumor activity at single dose as low as 300 µg/kg in mice, while maintaining tolerability at single dose of 20 – 30 mg/kg in rats. In contrast to both GO and lintuzumab vedotin, GLK-33 exhibited a wide therapeutic window and activity against multidrug-resistant cells. The development of GLK-33 addresses the limitations of previous ADCs, offering a wider therapeutic window, improved tolerability, and activity against drug-resistant leukemia cells. These findings encourage further exploration of GLK-33 in AML through clinical trials.

Introduction

Siglec-3 (CD33; sialic acid-binding Ig-like lectin 3) is a marker of myeloid cells expressed on malignant cells in about 90% of AML patients (1). It is present in leukemia stem cells but absent from hematopoietic stem cells (2). Anti-CD33 antibodies such as lintuzumab (LN) were found to be well tolerated but had limited efficacy in AML patients (3). GO, a potent anti-CD33 calicheamicin ADC, was initially approved for AML in 2000 with activity both as a single compound and in combination treatments (4). However, due to unacceptable toxicities caused by the combination of an unstable linker and a very potent payload, GO was temporarily withdrawn from the market between 2010 – 2017 (4). Currently, GO is administered with fractionated dosing, and it has been shown to significantly reduce the risk of relapse in patients with favorable cytogenetics, but not in high-risk patients with adverse karyotype (5). After the clinical validation of the therapeutic target by GO, new anti-CD33 ADCs have been developed, but with little success. AVE9633 carried low-potency maytansinoid payloads and had a more favorable safety profile than GO, but failed to show clinical activity (6). SGN-33A was based on highly potent pyrrolobenzodiazepine dimer (PBD) payloads and, unlike GO, was active against multi-drug resistant (MDR+) leukemia cells (7). However, SGN-33A showed severe toxicities and was discontinued. To date, anti-CD33 ADCs with a wider therapeutic window than GO are still lacking.

We have previously developed a new auristatin ADC payload MMAU (8), which is a hydrophilic glucuronide prodrug of the potent tubulin inhibitor monomethylauristatin E (MMAE). Further, we have recently developed an optimized hydrophilic glycopeptide linker with superior systemic stability, pharmacokinetics, *in vivo* efficacy, and tolerability (9). The novel linker-payload, mavg-MMAU, was conjugated to LN, which is an IgG1 antibody with strong Fc effector functions in

contrast to the IgG4 antibody gemtuzumab (10). The resulting ADC, GLK-33, showed excellent *in vivo* anti-leukemia activity and tolerability, wide therapeutic window, and activity against drug-resistant leukemia cells.

Methods

ADC generation

Palivizumab (Synagis) and GO (Mylotarg) were obtained commercially. LN was produced in-house in CHO cells using the ExpiCHO™ Expression System (Thermo Fisher Scientific) and the published amino acid sequence (11). Vedotin (mcvc-MMAE) was purchased from Levena Biopharma and maleimidoacetyl-β-Ala-Val-Ser(β-Glc)-para-aminobenzylcarbamate-monomethylauristatin U (mavg-MMAU (9)) was manufactured at SyntaBio LLC (San Diego, CA, USA). DAR8 ADCs were generated by reducing the four interchain disulfide bonds with 20x molar excess tris(2-carboxyethyl)phosphine (TCEP) to monoclonal antibody (mAb) and incubating for 1 hour at +37°C (8,9). 28x molar excess of maleimide-linker payload was added and incubated for 1 hour at +37°C (8). DAR4 ADCs were generated by limiting the reduction step by using 4x molar excess of TCEP followed by the linker-payload addition (9).

Antibodies and ADCs were purified by protein A affinity chromatography using HiTrap MabSelect Sure column and Äkta HPLC purifier system (Cytiva). The sample was loaded and the column washed with PBS. 0.1 M citrate pH 3 was used for elution, after which the buffer was exchanged to PBS using HiTrap Desalting column (Cytiva). The purified samples were sterile filtered. Maleimidoacetyl-linker conjugates were stabilized by incubation at +37°C overnight. Stabilization

was confirmed by MALDI-TOF mass spectrometric detection of 18 Da mass increase of the payload-conjugated light chain (9). Analytical methods are described in Supplementary Methods.

In vitro cytotoxicity assays

HL-60, MV4-11, K562, Ramos, Daudi (ATCC), MOLM-13, KG-1, and OCI-M1 (DSMZ) cells were cultured according to the cell suppliers' instructions. For toxicity assays, 6000-15000 cells/well were plated in 96-well plates. Serial dilutions of test compounds were added to triplicate or quintuplicate wells, and plates were incubated for 3-5 days at +37°C. Cell control was untreated cells in culture medium. The viability was measured with 2-4 hours incubation with PrestoBlue cell viability reagent (Life Technologies). Soluble human CD33 protein (sCD33) was from Sino Biological. ADCC and CDC assay procedures are described in Supplementary Methods. Dose-response curves and IC50 values were obtained by four parameter logistic regression analysis using GraphPad Prism 9.1.5.

Ex vivo drug sensitivity of primary AML samples

Six AML patient samples were obtained from the Helsinki University Hospital Comprehensive Cancer Center after informed consent (permit numbers 239/13/03/00/2010, 303/13/03/01/2011, Helsinki University Hospital Ethics Committee) and in compliance with the Declaration of Helsinki. Mononuclear cells were isolated by Ficoll gradient centrifugation and vitally frozen in fetal bovine serum with 5% dimethyl sulfoxide until tested in the *ex vivo* assays. Details of the assays are provided in the Supplementary Methods and as previously described (12).

Metabolic assays

Incubations with microsome preparates from human, Sprague-Dawley rat, cynomolgus monkey, and Göttingen mini-pig liver (tebu-bio) were performed at +37°C in 50 mM sodium acetate pH 4.5.

Animal models

Studies with HL-60 and MOLM-13 xenografts were performed at the Turku Center for Disease Modeling (TCDM), University of Turku, Finland, according to the rules of Council of Europe and National Research Council, USA, and approval by the Finnish Animal Experiment Board. The single-dose non-GLP rat tolerability study was performed at the Central Animal Laboratory, University of Turku, Finland, according to appropriate international guidelines and ethical committee approval by the National Project Authorization Board of Finland (Care and Use Committee). Experiment details are described in Supplementary Methods.

Data sharing statement

For original data, please contact the corresponding authors.

Results

Generation and characterization of a homogeneous lintuzumab-auristatin conjugate

GLK-33 with a drug-to-antibody ratio of 8 (DAR8) was prepared by reducing all the four hinge

disulfides of LN and conjugating the cysteine side chains with the mavg-MMAU linker-payload (Figure 1A). GLK-33 was highly homogeneous as judged by MALDI-TOF mass spectrometry, SEC-, HIC- and RP-HPLC (Figure 1B-E). A comparator ADC, lintuzumab vedotin (LV), was generated using the mcvc-MMAE linker-payload and limiting the reduction step so that an average of two disulfides were reduced, resulting in a mixture of DAR0-8 species with on average DAR4 (Supplementary Figure 1), similarly as with approved MMAE ADCs (13). GLK-33 was efficiently bound and internalized to CD33+ leukemia cells (Supplementary Figure 2). Like previously reported (14), LN, the antibody component of GLK-33, did not bind to either monkey or mouse CD33-Fc fusion proteins (Figure 2A). GLK-33 and LN had comparable binding affinities to recombinant human CD33 and CD33-Fc in ELISA (Figure 2B, EC50 between 200-400 pM).

In vitro cytotoxicity against leukemia cell lines

GLK-33 cytotoxicity experiments were performed with six leukemia cell lines with variable CD33 surface expression levels, as well as two CD33-negative lymphoma cell lines (Figure 2C, Supplementary Table 1). The inhibitory concentrations that reduced cell viability by 50% (IC50) ranged from 140 pM to 2.7 nM, except for 725 nM against the CD33-low cell line K-562. The specificity of the cytotoxic activity of GLK-33 against CD33 was shown with relevant controls, as exemplified with the leukemia cell line MOLM-13 (Figure 2D). The IC50 was picomolar for GLK-33, whereas a non-binding isotype control ADC with the same linker-payload and DAR, palivizumab-mavg-MMAU DAR8, had about 1000-fold higher IC50. The free payload MMAU had an IC50 of over 200 nM and LN had no activity.

Next, we compared the cytotoxicity of GLK-33 to comparator ADCs LV and GO. In HL-60 cells,

GLK-33 had 19-fold higher activity than LV (Figure 2E) but 40-fold lower than GO (Figure 2F). However, GLK-33 did not have any cytotoxicity to CD33-negative Daudi lymphoma cells even at 1 μM concentration, whereas GO showed low-nanomolar off-target cytotoxicity (Figure 2F). Importantly, GLK-33 was markedly more cytotoxic than GO against KG-1 AML cells (Figure 2F). The resistance of KG-1 cells to GO is caused by their MDR+ status and is reversible by the P-glycoprotein/MDR1 inhibitor verapamil (15). Consistent with this, in the presence of 5 μM verapamil, GO had low-nanomolar IC50 against KG-1 cells, whereas IC50 was not reached without verapamil even at 100 nM GO (Figure 2G). Similarly, LV showed over 100-fold reduction in IC50 against KG-1 cells when verapamil was used (Figure 2H). However, the activity of GLK-33 against KG-1 cells was increased only 3-fold with the addition of verapamil (Figure 2I). Taken together, GLK-33 showed potent and target-specific cytotoxic activity against CD33+ leukemia cell lines and was markedly more potent against MDR+ cells than either LV or GO.

Antibody effector functions

LN has been shown to elicit both antibody-dependent cellular cytotoxicity (ADCC) and complement-dependent cytotoxicity (CDC), which were suggested to have a major role in the clinical anti-leukemia activity of the naked antibody (16). In ADCC assays with natural killer (NK) cells from human donors (Figure 2J), GLK-33 showed target-specific ADCC activity with EC50 of 5 nM. The activity was Fc receptor-dependent since there was no target cell lysis after enzymatic deglycosylation of GLK-33. However, GLK-33 had 17-fold lower ADCC activity than LN, while LV had only 2-fold lower activity than LN. Further, GLK-33 had CDC-inducing activity against HL-60 cells using rabbit serum as the complement donor, but several-fold less than LN (Figure 2K). In conclusion, GLK-33 showed both ADCC and CDC at clinically relevant concentrations, but its Fc effector functions were

attenuated compared to both LN and LV.

Negligible inhibition by soluble CD33

CD33 may be shed from leukemia cells *in vivo* and the resulting soluble CD33 (sCD33) can be found in bone marrow plasma at concentrations between 0.4 – 30 ng/mL (17), which might interfere with target cell binding and cytotoxicity of an ADC. However, the IC50 of GLK-33 against HL-60 cells was only marginally increased with 100 ng/mL sCD33 added to the assay (Figure 2L), with full efficacy at clinically relevant >10 nM concentrations of GLK-33.

Ex vivo cytotoxicity against patient-derived leukemia blasts

Next, we evaluated the efficacy of GLK-33 using six primary AML patient samples with CD33-positive blasts (Supplementary Table 1). Patient mononuclear cells were exposed to GLK-33, LN, MMAU, and GO for five days, after which the remaining viable blast cells were quantified using flow cytometry. GLK-33 was effective at targeting blasts with a median IC50 of 16 nM (Figure 3A, Supplementary Figure 3A). In contrast, both LN and MMAU displayed only modest activity against blasts, similarly as observed in the leukemia cell lines. GO demonstrated high efficacy against the blasts, with a median IC50 of 0.3 nM (Figure 3A). Subsequently, we assessed toxicity against lymphocytes (CD33-negative) in the same samples. GLK-33, LN, and MMAU did not exhibit cytotoxic activity against lymphocytes, while GO displayed significant lymphocyte toxicity across all samples (median IC50 of 9 nM; Figure 3B, Supplementary Figure 3B). These results indicate that GLK-33 has potent activity against patient-derived blasts and does not demonstrate off-target lymphocyte toxicity in contrast to GO.

In vivo anti-leukemia efficacy

Anti-tumor efficacy of GLK-33 was evaluated in subcutaneous (*s.c.*) xenograft models in mice (Figure 4). A single 3 mg/kg *i.v.* dose of both GLK-33 and LV led to the disappearance of HL-60 xenograft tumors in all mice (100% complete responses, CR), whereas 10 mg/kg LN and 3 mg/kg palivizumab-mavg-MMAU DAR8 (isotype ADC) only modestly inhibited tumor growth (Figure 4A, high dose). Also 1 mg/kg dose of GLK-33 removed the tumors in all mice (100% CR), in contrast to 1 mg/kg dose of LV (33% CR; Figure 4A, middle dose; Figure 4C). With the lowest dose of 300 µg/kg, GLK-33 inhibited tumor growth (Figure 4A, low dose), and sustained responses to the end of the study in three of six mice (50% CR), in contrast to LV (17% CR; Figure 4C). Figure 4B shows comparison of individual tumor volumes on day 39 after tumor inoculation. GLK-33 significantly inhibited tumor growth compared to vehicle control down to 300 µg/kg single dose, whereas LV showed significant tumor growth inhibition only at 1 mg/kg dose. The higher activity of GLK-33 over LV was also visible in the progression-free survival curves at the middle and low dose levels (Figure 4C). Taken together, GLK-33 had about 3-fold higher *in vivo* anti-leukemia activity than LV in the HL-60 xenograft tumor model.

The ADC concentration of LV decreased rapidly following the administration and was 8-fold lower than GLK-33 ADC concentration after seven days, in accordance to the known *in vivo* instability of the vedotin linker (18). In contrast to LV, the ADC concentration of GLK-33 did not fall relative to the total antibody concentration, demonstrating higher linker stability and 4-fold improved systemic ADC exposure and terminal half-life compared to LV (Supplementary Table 2).

GLK-33 was further evaluated in another mouse model with *s.c.* MOLM-13 xenograft tumors (Figure 4E-F). A single 3 mg/kg dose of GLK-33 eradicated the tumors in all mice (100% CR), whereas 10 mg/kg LN and 3 mg/kg isotype ADC showed only minor tumor growth inhibition (Figure 4E, high

dose). At middle and low dose levels, GLK-33 showed dose-dependent activity (Figure 4E, middle/low dose). GLK-33 significantly inhibited tumor growth down to 300 µg/kg single dose compared to vehicle control (Figure 4F). In conclusion, GLK-33 had potent, target-specific *in vivo* anti-leukemia tumor activity at single dose down to 300 µg/kg.

ADC metabolism

The cytotoxic activity of auristatin ADCs requires that the active payload MMAE or linker-payload metabolite (19) is liberated to the target cell causing tubulin inhibition and apoptosis. We have previously shown that ADCs with the mavg-MMAU payload i) liberate both MMAE and Cys-mavg-MMAE metabolites when the ADC is metabolized by both rat and human lysosomal enzymes, ii) the final metabolite is MMAE, and iii) the rate of metabolism is slower than that of vedotin ADCs (Figure 5A; Goldberg *et al.* submitted). Here, GLK-33 was incubated *in vitro* with human, rat, cynomolgus monkey, and pig liver microsomal preparates at the nominal lysosomal pH of 4.5 (Figure 5B). Analysis of the resulting ADC and payload fragments by MALDI-TOF mass spectrometry revealed that the metabolic pathways in the liver microsomal preparates were overall similar across species (Figure 5B). The glucuronide detached first (fragment L1) and free MMAE (metabolite P1) appeared as the final metabolite in all four species. However, in the present study, Cys-mavg-MMAE (metabolite P2) was detected only in rat liver microsome preparates that had the highest metabolic activity. Very slow β-glucosidase activity, cleaving the glucose off the glucoserine residue, was previously detected with rat and human lysosomal preparates (Goldberg *et al.* submitted), but it was not detected here with the liver microsome preparates.

ADC toxicity and toxicokinetics in rats

The initial safety of GLK-33 was evaluated in a single dose tolerability and toxicokinetic study in Sprague-Dawley rats (Figure 6). ~~LN and GLK-33 do not cross-react with rodent CD33 (ref. (14) and Figure 2A) and the observations thus show off-target toxicities.~~ Study design and toxicology findings are described in Figure 6A. The ADC was well tolerated at doses of 10 – 20 mg/kg. The maximum tolerated dose (MTD) was between 20 – 30 mg/kg. ADC-related hematological changes were not observed until decreases in the amounts of white blood cells and platelets at ≥30 mg/kg doses, as well as decreases in red blood cells and hemoglobin at 40 mg/kg dose. Changes to clinical chemistry parameters included increases in alanine aminotransferase (ALT; marker for liver toxicity) and amylase (pancreatic toxicity) at ≥30 mg/kg doses, as well as a decrease in the albumin-to-globulin ratio (liver toxicity) at 40 mg/kg dose. ADC-related organ weight changes included decreased thymic weights (immune cell depletion) at ≥30 mg/kg doses. The effects were qualitatively similar, but milder, and occurred at higher doses compared to vedotin ADCs (20,21).

Following the administration of GLK-33, plasma levels of the ADC, total human antibody and free MMAE were quantitated (Figure 6B-C), while free MMAU levels were below the limit of quantitation. ADC and total antibody exposures were comparable, indicating high *in vivo* linker stability. This was verified by immunoaffinity isolation and mass spectrometric analysis of the ADC from rat plasma samples, showing that there was no detectable loss of linker-payload during at least nine days in circulation (Figure 6D). The free payload MMAU was well tolerated in rat at the highest administered dose of 2.55 mg/kg (Supplementary Data).

Discussion

The present report describes the preclinical evaluation of a novel ADC drug candidate against AML. GLK-33 is composed of LN, a clinically validated humanized anti-CD33 monoclonal antibody, conjugated to the potent auristatin family payload MMAU, a glucuronide prodrug of MMAE with increased hydrophilicity (8). We achieved a homogeneous drug loading of eight mavg-MMAU linker-payloads per antibody (DAR8) unlike the majority of currently approved ADCs that have on average DAR4 and are heterogeneous mixtures of DAR0-8 components (22). Similarly, GO comprises up to 50% of unconjugated antibody (23,24) that can block CD33 receptors from ADC internalization. The ability to generate DAR8 auristatin ADCs while increasing *in vivo* efficacy and tolerability surpasses the utility of the vedotin linker-payload (mcvc-MMAE). Homogeneous ADCs have been shown to have higher efficacy, better tolerability and wider therapeutic window than their heterogeneous counterparts (25).

The DAR8 approach allows for delivery of high amounts of cytotoxic compounds to target cells. Although CD33 is generally overexpressed in AML, it is a medium copy number target with about 10^5 copies/cell in AML patients (26). The highly potent ADCs GO and SGN-33A both demonstrated efficacy in AML patients, while AVE9633, a DAR4 ADC utilizing the less-potent payload DM4, failed to show clinical activity even at super-saturating doses (6). GLK-33 showed high efficacy against several leukemia cell lines *in vitro* and was not inhibited by soluble CD33 at physiological concentrations. GLK-33 was active against patient-derived CD33+ AML blasts in *ex vivo* assays with IC50 values between 200 pM – 211 nM, which is within the clinical C_{max} of the anti-CD30 ADC brentuximab vedotin (BV) at 1.8 mg/kg dose (27). GLK-33 showed significant anti-tumor activity down to 300 μg/kg single dose in two xenograft tumor models. The present evidence thus suggests

suitable efficacy potential for GLK-33. Further, GLK-33 was shown capable of eliciting both ADCC and CDC against leukemia cells at clinically relevant concentrations, however with attenuated efficacy compared to both LN and LV. Relative importance of Fc receptor-mediated effects to on-target efficacy and off-target toxicity is currently under discussion in the ADC field (28,29), and the unconjugated antibody LN failed to show significant therapeutic effect in phase 3 clinical trials (30).

A known weakness of GO is its poor clinical efficacy against drug-resistant AML, especially disease with MDR-associated P-glycoprotein expression (31,32), which is detected in ~40% of AML patients (33). In addition to GO (15), also LV was poorly efficacious against MDR+ cells without co-treatment with P-glycoprotein inhibitor, consistent with the known sensitivity of MMAE to drug efflux pumps (34). In contrast, GLK-33 was active against the MDR+ cells. The ability of GLK-33 to overcome drug resistance by drug efflux pump activity is an important advantage over GO and vedotin ADCs. We hypothesize that the slow release of MMAE from mavg-MMAU linker-payload may form a long-lasting lysosomal stock of payload to counteract drug efflux from a cytosolic stock of payload not bound by tubulin (35). Further, in contrast to vedotin, a poorly membrane-permeable metabolite (Cys-mavg-MMAE) was also formed during GLK-33 metabolism. However, further studies are needed to establish the relative importance of the slow payload release and the hydrophilic metabolite in the increased ability of GLK-33 to counteract drug resistance.

The major disadvantage of GO is its problematic toxicity profile, notably liver and hematologic toxicity as well as risk for veno-occlusive disease, which led to its temporary withdrawal from the market during 2010 – 2017 (4). GO's reapproval was based on improved safety and retained efficacy after halving the clinical dose with fractionated dosing, from two 9 mg/m^2 doses on days 1 and 15 of induction therapy to three 3 mg/m^2 doses on days 1, 4 and 7 (32,36). While the 9 mg/m^2 dose had shown optimal saturation of CD33 in PB blasts (37), fractionated dosing was hypothesized to improve

overall drug internalization to target cells (32,38). However, the *in vivo* saturation of CD33 in BM blasts was insufficient already at the 9 mg/m^2 dose level (39). In contrast to GO, multiple cycles of both AVE9633 and SGN-33A were dosed in clinical trials to sustain the therapeutic dose for a longer time, and patients who responded to treatment were given over ten cycles with acceptable toxicity (6,40). GLK-33 had single dose rat MTD of 20 – 30 mg/kg, which is about 15-fold higher than that of GO (1.4 – 2 mg/kg (36)). The preclinical therapeutic index (TI) of GLK-33, based on conversion to the human equivalent dose (41), is between 130 – 200, whereas the TI of GO is between 3 – 4. The present results suggest that off-target toxicities should not prohibit dosing of GLK-33 to fully saturating levels. The most likely adverse events may instead be caused by on-target toxicity to myeloid cells, similar to other CD33-targeting agents (40,42).

The overall toxicity profile of GLK-33 was similar to vedotin ADCs in rat, although shifted to higher doses, including bone marrow, liver and gastrointestinal tract toxicity (20,21). The MTD is high compared to vedotin ADCs, which are DAR4 ADCs in contrast to GLK-33. For example, the single dose rat MTD of BV was 15 mg/kg (21), and thus GLK-33 showed over 2.5-fold higher tolerability than BV per amount of delivered payload (Supplementary Figure 4A). The favorable rat tolerability result is not directly indicative of potential for high human dose, where there might be a risk for bystander toxicity in the bone marrow due to potentially increased target-mediated disposition. No cross-reactive species has thus far been identified for either LN or GLK-33. Mouse and rat CD33 sequences have only 49% – 53% amino acid sequence identity with human CD33, respectively, whereas cyno and human CD33 amino acid sequences have 87% identity. We did not perform binding assays with rat CD33. However, no evidence of on-target myelotoxicity was observed in the rat tolerability study, and rats administered with GLK-33 showed markedly less toxicity on leukocytes, thrombocytes and erythrocytes than comparable doses of vedotin ADCs. The dose of BV and the

other approved vedotin ADCs is generally limited by off-target toxicities (43) due to linker instability (18) and payload hydrophobicity (44) to between 1.5 – 2.5 mg/kg in human patients (20,45). GLK-33 was shown to release MMAE as its final metabolite. Vedotin ADCs have demonstrated that MMAE has a mild toxicity profile, has the advantage of bystander cell kill activity (34), and combines effectively with checkpoint inhibitor therapies (46–48). GLK-33 improved both the efficacy and the tolerability aspects of the TI of vedotin ADCs (Supplementary Figure 4B), plausibly due to its higher linker stability and the improved terminal half-life and systemic exposure.

Despite recent advances in molecularly targeted therapies such as FLT3 (49) and BCL-2 inhibitors (50), the standard chemotherapy for AML has remained the same since 1973 (51). In the United States alone, over 20,000 new AML cases and over 11,000 deaths from AML are expected in 2023. Five-year survival rates for AML are below 30%, with significantly poorer outcomes observed in older patients due to lower tolerance for intensive chemotherapy and higher prevalence of drug resistance (52). Therefore, there is a need for more efficacious and better-tolerated therapeutics for AML. GO is used to treat only a fraction of AML patients with favorable cytogenetic risk disease (53), although CD33 expression itself is associated with poor prognosis (54). An effective anti-CD33 ADC combining a good safety profile with activity against drug-resistant disease, such as GLK-33, could be an attractive treatment option for both GO-eligible and wider patient populations. Mutations that are associated with increased expression of CD33, including NPM1 (55) and FLT3 (54), could be used to select patients that could benefit the most from CD33-targeted therapy for clinical trials. GLK-33, like LN and GO, does not bind to the D2-CD33 splice variant of CD33, which could be used for further selection of AML patients (56). CD33 overexpression occurs also in other hematologic diseases (57–59), and GO as well as other CD33-targeting agents have been evaluated in acute promyelocytic leukemia (60,61), multiple myeloma (62), and myelodysplastic syndrome (63),

however without drug approvals to date.

In conclusion, the present study demonstrated broad-spectrum activity of GLK-33 in diverse models of CD33+ leukemia both *in vitro* and *in vivo*. GLK-33 has homogeneous high-DAR ADC design, and it showed high potency, ability to overcome drug resistance, excellent pharmacokinetics, and favorable off-target toxicity profile. These findings provide a scientific basis for clinical studies evaluating the safety and efficacy of GLK-33 in AML patients.

Acknowledgements

We thank Petra Sipilä, Nina Messner, Katri Hovirinta, Heli Niittymäki, Janne Sulku, and Suvi Luomala at the Turku Center for Disease Modeling (TCDM), as well as Joonas Khabbal and Mikko Voipio at the Central Animal Laboratory, University of Turku, Finland, for excellent performance of the animal studies. Metabolomics analyses were carried out at the FIMM Metabolomics Unit, which is hosted by the University of Helsinki and supported by HiLIFE and Biocenter Finland. This study was supported (in part) by research funding to MK from Finnish Medical Foundation, Cancer Foundation Finland and Sohlberg Foundation.

Authorship Contributions

Conception and design: TS, JS

Data acquisition: HP, OA, AH, VP, TL, TK, RN, ALH, IV, RR

Analysis and interpretation of data: TS, HP, OA, JOH, AH, VP, TL, TK, RN, ALH, JH, HK, IV, RR, AIN, CAH, MK, JS

All authors participated in the writing, review, and/or revision of the manuscript.

Disclosure of Conflicts of Interest

TS, HP, OA, JOH, VP, TL, TK, AH, ALH, RN, JH and JS are employees and/or shareholders of Glykos Finland Oy. TS, HP, OA, JH, and JS are inventors in patents/applications directed to the technology. MK reports personal fees (Astellas Pharma, AbbVie, Bristol-Myers Squibb, Faron Pharmaceuticals, Jazz Pharmaceuticals, Novartis and Servier) and research funding from AbbVie (outside the submitted work). CAH has research funding from Kronos Bio, Novartis, Oncopeptides, WNTResearch, and Zentalis Pharmaceuticals, plus personal fees from Autolus, all unrelated to the submitted work.

References

1. Molica M, Perrone S, Mazzone C, Niscola P, Cesini L, Abruzzese E, et al. CD33 Expression and Gentuzumab Ozogamicin in Acute Myeloid Leukemia: Two Sides of the Same Coin. Cancers. 2021;13:3214.

2. Hauswirth AW, Florian S, Printz D, Sotlar K, Krauth M-T, Fritsch G, et al. Expression of the target receptor CD33 in CD34+/CD38-/CD123+ AML stem cells. Eur J Clin Invest. 2007;37:73–82.

3. Lancet JE, Sekeres MA, Wood BL, Grove LE, Sandalic L, Sievers EL, et al. Lintuzumab and Low-Dose Cytarabine Compared to Placebo and Low-Dose Cytarabine in Patients with Untreated Acute Myeloid Leukemia (AML) 60 Years and Older: Results of a Randomized, Double-Blinded Phase 2b Study,. Blood. 2011;118:3613.

4. Ali S, Dunmore H-M, Karres D, Hay JL, Salmonsson T, Gisselbrecht C, et al. The EMA Review of Mylotarg (Gemtuzumab Ozogamicin) for the Treatment of Acute Myeloid Leukemia. The Oncologist. 2019;24:e171–9.

5. Hills RK, Castaigne S, Appelbaum FR, Delaunay J, Petersdorf S, Othus M, et al. Addition of gemtuzumab ozogamicin to induction chemotherapy in adult patients with acute myeloid leukaemia: a meta-analysis of individual patient data from randomised controlled trials. Lancet Oncol. 2014;15:986–96.

6. Lapusan S, Vidriales MB, Thomas X, de Botton S, Vekhoff A, Tang R, et al. Phase I studies of AVE9633, an anti-CD33 antibody-maytansinoid conjugate, in adult patients with relapsed/refractory acute myeloid leukemia. Invest New Drugs. 2012;30:1121–31.

7. Kung Sutherland MS, Walter RB, Jeffrey SC, Burke PJ, Yu C, Kostner H, et al. SGN-CD33A: a novel CD33-targeting antibody-drug conjugate using a pyrrolobenzodiazepine dimer is active in models of drug-resistant AML. Blood. 2013;122:1455–63.

8. Satomaa T, Pynnönen H, Vilkman A, Kotiranta T, Pitkänen V, Heiskanen A, et al. Hydrophilic Auristatin Glycoside Payload Enables Improved Antibody-Drug Conjugate Efficacy and Biocompatibility. Antibodies. 2018;7:15.

9. Goldberg S, Satomaa T, Aina O, Aitio O, Burke K, Dudkin V, et al. Trastuzumab-MMAU antibody-auristatin conjugates: Valine-glucoserine linker with stabilized maleimide conjugation improves in vivo efficacy and tolerability. Mol Cancer Ther. 2024;

10. Vidarsson G, Dekkers G, Rispens T. IgG subclasses and allotypes: from structure to effector functions. Front Immunol. 2014;5:520.

11. INN Proposed List 121. WHO Drug Information, Vol. 33, No. 4, 2019. [Internet]. [cited 2023 Nov 22]. Available from: https://www.who.int/publications/m/item/inn-pl-121

12. Kuusanmäki H, Leppä A-M, Pölönen P, Kontro M, Dufva O, Deb D, et al. Phenotype-based drug screening reveals association between venetoclax response and differentiation stage in acute myeloid leukemia. Haematologica. 2020;105:708–20.

13. Sarrut M, Fekete S, Janin-Bussat M-C, Colas O, Guillarme D, Beck A, et al. Analysis of antibody-drug conjugates by comprehensive on-line two-dimensional hydrophobic interaction chromatography x

reversed phase liquid chromatography hyphenated to high resolution mass spectrometry. II- Identification of sub-units for the characterization of even and odd load drug species. J Chromatogr B. 2016;1032:91–102.

14. Miederer M, McDevitt MR, Sgouros G, Kramer K, Cheung N-KV, Scheinberg DA. Pharmacokinetics, dosimetry, and toxicity of the targetable atomic generator, 225Ac-HuM195, in nonhuman primates. J Nucl Med. 2004;45:129–37.

15. Inase A, Maimaitili Y, Kimbara S, Mizutani Y, Miyata Y, Ohata S, et al. GSK3 inhibitor enhances gemtuzumab ozogamicin-induced apoptosis in primary human leukemia cells by overcoming multiple mechanisms of resistance. EJHaem. 2022;4:153–64.

16. Sutherland MK, Yu C, Lewis TS, Miyamoto JB, Morris-Tilden CA, Jonas M, et al. Anti-leukemic activity of lintuzumab (SGN-33) in preclinical models of acute myeloid leukemia. mAbs. 2009;1:481–90.

17. Biedermann B, Gil D, Bowen DT, Crocker PR. Analysis of the CD33-related siglec family reveals that Siglec-9 is an endocytic receptor expressed on subsets of acute myeloid leukemia cells and absent from normal hematopoietic progenitors. Leuk Res. 2007;31:211–20.

18. Hinrichs MJM, Dixit R. Antibody Drug Conjugates: Nonclinical Safety Considerations. AAPS J. 2015;17:1055–64.

19. Caculitan NG, dela Cruz Chuh J, Ma Y, Zhang D, Kozak KR, Liu Y, et al. Cathepsin B Is Dispensable for Cellular Processing of Cathepsin B-Cleavable Antibody–Drug Conjugates. Cancer Res. 2017;77:7027–37.

20. Saber H, Leighton JK. An FDA oncology analysis of antibody-drug conjugates. Regul Toxicol Pharmacol. 2015;71:444–52.

21. Adcetris EPAR public assessment report [Internet]. [cited 2023 Apr 21]. Available from: https://www.ema.europa.eu/en/documents/assessment-report/adcetris-epar-public-assessment-report_en.pdf

22. Fu Z, Li S, Han S, Shi C, Zhang Y. Antibody drug conjugate: the “biological missile” for targeted cancer therapy. Signal Transduct Target Ther. 2022;7:1–25.

23. Bross PF, Beitz J, Chen G, Chen XH, Duffy E, Kieffer L, et al. Approval summary: gemtuzumab ozogamicin in relapsed acute myeloid leukemia. Clin Cancer Res Off J Am Assoc Cancer Res. 2001;7:1490–6.

24. Labrijn AF, Buijsse AO, van den Bremer ETJ, Verwilligen AYW, Bleeker WK, Thorpe SJ, et al. Therapeutic IgG4 antibodies engage in Fab-arm exchange with endogenous human IgG4 in vivo. Nat Biotechnol. 2009;27:767–71.

25. Kline T, Steiner AR, Penta K, Sato AK, Hallam TJ, Yin G. Methods to Make Homogenous Antibody Drug Conjugates. Pharm Res. 2015;32:3480–93.

26. Jilani I, Estey E, Huh Y, Joe Y, Manshouri T, Yared M, et al. Differences in CD33 intensity between various myeloid neoplasms. Am J Clin Pathol. 2002;118:560–6.

27. Adcetris PMDA deliberation results [Internet]. [cited 2023 Jun 12]. Available from:

https://www.pmda.go.jp/files/000243154.pdf

28. Aoyama M, Tada M, Yokoo H, Demizu Y, Ishii-Watabe A. Fcγ Receptor-Dependent Internalization and Off-Target Cytotoxicity of Antibody-Drug Conjugate Aggregates. Pharm Res. 2022;39:89–103.

29. Tai Y-T, Mayes PA, Acharya C, Zhong MY, Cea M, Cagnetta A, et al. Novel anti-B-cell maturation antigen antibody-drug conjugate (GSK2857916) selectively induces killing of multiple myeloma. Blood. 2014;123:3128–38.

30. Feldman EJ, Brandwein J, Stone R, Kalaycio M, Moore J, O'Connor J, et al. Phase III randomized multicenter study of a humanized anti-CD33 monoclonal antibody, lintuzumab, in combination with chemotherapy, versus chemotherapy alone in patients with refractory or first-relapsed acute myeloid leukemia. J Clin Oncol Off J Am Soc Clin Oncol. 2005;23:4110–6.

31. Walter RB, Gooley TA, van der Velden VHJ, Loken MR, van Dongen JJM, Flowers DA, et al. CD33 expression and P-glycoprotein-mediated drug efflux inversely correlate and predict clinical outcome in patients with acute myeloid leukemia treated with gemtuzumab ozogamicin monotherapy. Blood. 2007;109:4168–70.

32. Taksin A-L, Legrand O, Raffoux E, de Revel T, Thomas X, Contentin N, et al. High efficacy and safety profile of fractionated doses of Mylotarg as induction therapy in patients with relapsed acute myeloblastic leukemia: a prospective study of the alfa group. Leukemia. 2007;21:66–71.

33. Seedhouse CH, Grundy M, White P, Li Y, Fisher J, Yakunina D, et al. Sequential influences of leukemia-specific and genetic factors on p-glycoprotein expression in blasts from 817 patients entered into the National Cancer Research Network acute myeloid leukemia 14 and 15 trials. Clin Cancer Res. 2007;13:7059–66.

34. Moquist PN, Bovee TD, Waight AB, Mitchell JA, Miyamoto JB, Mason ML, et al. Novel Auristatins with High Bystander and Cytotoxic Activities in Drug Efflux-positive Tumor Models. Mol Cancer Ther. 2021;20:320–8.

35. Hong EE, Erickson H, Lutz RJ, Whiteman KR, Jones G, Kovtun Y, et al. Design of Coltuximab Ravtansine, a CD19-Targeting Antibody–Drug Conjugate (ADC) for the Treatment of B-Cell Malignancies: Structure–Activity Relationships and Preclinical Evaluation. Mol Pharm. 2015;12:1703–16.

36. Mylotarg EPAR public assessment report [Internet]. [cited 2023 Aug 25]. Available from: https://www.ema.europa.eu/en/documents/assessment-report/mylotarg-epar-public-assessment-report_en.pdf

37. Sievers EL, Appelbaum FR, Spielberger RT, Forman SJ, Flowers D, Smith FO, et al. Selective Ablation of Acute Myeloid Leukemia Using Antibody-Targeted Chemotherapy: A Phase I Study of an Anti-CD33 Calicheamicin Immunoconjugate. Blood. 1999;93:3678–84.

38. van der Velden VHJ, te Marvelde JG, Hoogeveen PG, Bernstein ID, Houtsmuller AB, Berger MS, et al. Targeting of the CD33-calicheamicin immunoconjugate Mylotarg (CMA-676) in acute myeloid leukemia: in vivo and in vitro saturation and internalization by leukemic and normal myeloid cells. Blood. 2001;97:3197–204.

39. van der Velden VHJ, Boeckx N, Jedema I, te Marvelde JG, Hoogeveen PG, Boogaerts M, et al. High CD33-antigen loads in peripheral blood limit the efficacy of gemtuzumab ozogamicin (Mylotarg) treatment in

acute myeloid leukemia patients. Leukemia. 2004;18:983–8.

40. Stein EM, Walter RB, Erba HP, Fathi AT, Advani AS, Lancet JE, et al. A phase 1 trial of vadastuximab talirine as monotherapy in patients with CD33-positive acute myeloid leukemia. Blood. 2018;131:387–96.

41. Nair AB, Jacob S. A simple practice guide for dose conversion between animals and human. J Basic Clin Pharm. 2016;7:27–31.

42. Rosenblat TL, McDevitt MR, Carrasquillo JA, Pandit-Taskar N, Frattini MG, Maslak PG, et al. Treatment of Patients with Acute Myeloid Leukemia with the Targeted Alpha-Particle Nanogenerator Actinium-225-Lintuzumab. Clin Cancer Res. 2022;28:2030–7.

43. Nessler I, Menezes B, Thurber GM. Key metrics to expanding the pipeline of successful antibody-drug conjugates. Trends Pharmacol Sci. 2021;42:803–12.

44. Burke PJ, Hamilton JZ, Jeffrey SC, Hunter JH, Doronina SO, Okeley NM, et al. Optimization of a PEGylated Glucuronide-Monomethylauristatin E Linker for Antibody-Drug Conjugates. Mol Cancer Ther. 2017;16:116–23.

45. Deeks ED. Disitamab Vedotin: First Approval. Drugs. 2021;81:1929–35.

46. Müller P, Martin K, Theurich S, Schreiner J, Savic S, Terszowski G, et al. Microtubule-depolymerizing agents used in antibody-drug conjugates induce antitumor immunity by stimulation of dendritic cells. Cancer Immunol Res. 2014;2:741–55.

47. Hoimes CJ, Flaig TW, Milowsky MI, Friedlander TW, Bilen MA, Gupta S, et al. Enfortumab Vedotin Plus Pembrolizumab in Previously Untreated Advanced Urothelial Cancer. J Clin Oncol. Wolters Kluwer; 2023;41:22–31.

48. Cao A, Heiser R, Law C-L, Gardai SJ. Auristatin-based antibody drug conjugates activate multiple ER stress response pathways resulting in immunogenic cell death and amplified T-cell responses. Cancer Res. 2016;76:4914–4914.

49. Zhao JC, Agarwal S, Ahmad H, Amin K, Bewersdorf JP, Zeidan AM. A review of FLT3 inhibitors in acute myeloid leukemia. Blood Rev. 2022;52:100905.

50. Pollyea DA, Pei S, Stevens BM, Smith CA, Jordan CT. The Intriguing Clinical Success of BCL-2 Inhibition in Acute Myeloid Leukemia. Annu Rev Cancer Biol. 2021;5:277–89.

51. Yates JW, Wallace HJ, Ellison RR, Holland JF. Cytosine arabinoside (NSC-63878) and daunorubicin (NSC-83142) therapy in acute nonlymphocytic leukemia. Cancer Chemother Rep. 1973;57:485–8.

52. Sasaki K, Ravandi F, Kadia TM, DiNardo CD, Short NJ, Borthakur G, et al. De novo acute myeloid leukemia: A population-based study of outcome in the United States based on the Surveillance, Epidemiology, and End Results (SEER) database, 1980 to 2017. Cancer. 2021;127:2049–61.

53. Döhner H, Wei AH, Appelbaum FR, Craddock C, DiNardo CD, Dombret H, et al. Diagnosis and management of AML in adults: 2022 recommendations from an international expert panel on behalf of the ELN. Blood. 2022;140:1345–77.

54. Liu J, Tong J, Yang H. Targeting CD33 for acute myeloid leukemia therapy. BMC Cancer. 2022;22:24.

55. De Propris MS, Raponi S, Diverio D, Milani ML, Meloni G, Falini B, et al. High CD33 expression levels in acute myeloid leukemia cells carrying the nucleophosmin (NPM1) mutation. Haematologica. 2011;96:1548–51.

56. Lamba JK, Chauhan L, Shin M, Loken MR, Pollard JA, Wang Y-C, et al. CD33 Splicing Polymorphism Determines Gemtuzumab Ozogamicin Response in De Novo Acute Myeloid Leukemia: Report From Randomized Phase III Children's Oncology Group Trial AAML0531. J Clin Oncol Off J Am Soc Clin Oncol. 2017;35:2674–82.

57. Gorczyca W. Acute promyelocytic leukemia: four distinct patterns by flow cytometry immunophenotyping. Pol J Pathol. 2012;63:8–17.

58. Bruins WSC, Zweegman S, Mutis T, van de Donk NWCJ. Targeted Therapy With Immunoconjugates for Multiple Myeloma. Front Immunol. 2020;11.

59. Sanford D, Garcia-Manero G, Jorgensen J, Konoplev S, Pierce S, Cortes J, et al. CD33 is frequently expressed in cases of myelodysplastic syndrome and chronic myelomonocytic leukemia with elevated blast count. Leuk Lymphoma. 2016;57:1965–8.

60. Lancet JE, Moseley AB, Coutre SE, DeAngelo DJ, Othus M, Tallman MS, et al. A phase 2 study of ATRA, arsenic trioxide, and gemtuzumab ozogamicin in patients with high-risk APL (SWOG 0535). Blood Adv. 2020;4:1683–9.

61. Jurcic JG, DeBlasio T, Dumont L, Yao TJ, Scheinberg DA. Molecular remission induction with retinoic acid and anti-CD33 monoclonal antibody HuM195 in acute promyelocytic leukemia. Clin Cancer Res. 2000;6:372–80.

62. Levy MY, Cicic D, Bergonio G, Berger M. Trial in Progress: Phase I Study of Actinium-225 (225Ac)-Lintuzumab in Patients with Refractory Multiple Myeloma. Clin Lymphoma Myeloma Leuk. Elsevier; 2017;17:S329–30.

63. Daver N, Kantarjian H, Ravandi F, Estey E, Wang X, Garcia-Manero G, et al. A phase II study of decitabine and gemtuzumab ozogamicin in newly diagnosed and relapsed acute myeloid leukemia and high-risk myelodysplastic syndrome. Leukemia. 2016;30:268–73.

Figure Legends

Figure 1. Structure and characterization of GLK-33. **A.** Generation of GLK-33 by conjugating mavg-MMAU linker-payloads to the anti-CD33 monoclonal antibody lintuzumab (LN) with a drug-to-antibody ratio of eight (DAR8). *Red lines* between the antibody chains represent the hinge region cysteine disulfides, which were 1) reduced and 2) conjugated with the maleimide-activated linker-payloads (represented by *stars*), after which 3) the conjugated maleimides were stabilized by hydrolysis at physiological pH. For simplicity, only one hydrolyzed isomer is shown. *Black dots* between the antibody chains show the CH2 domain N-glycans. **B.** MALDI-TOF mass spectrometric analysis of GLK-33. *x-axis* shows m/z and *y-axis* shows relative signal intensity. *LC* = light chain detected as a singly charged ion $[LC+H]^{+}$. *HC* = heavy chain detected as a doubly charged ion $[HC+2H]^{2+}$. *PL* = maleimide-stabilized linker-payloads. **C.** Size-exclusion chromatography (SEC-HPLC) analysis. Aggregated high-molecular weight components (HMWC) elute before the monomeric ADC. **D.** Reversed phase chromatography (RP-HPLC) analysis. DAR was calculated based on integrated absorbances at 280 nm (y-axis). **E.** Hydrophobic interaction chromatography (HIC-HPLC) analysis.

Figure 2. *In vitro* evaluation of GLK-33. **A.-B.** CD33-binding assays of LN and GLK-33. Half-maximal effective concentrations (EC50) are shown. *x-axis* shows the concentration and *y-axis* shows the relative amount of bound antibody or ADC based on ELISA (absorbance at 450 nm). *Error bars* show the standard deviation. **A.** LN bound to human CD33 but not to either monkey or ~~rodent~~ mouse CD33. **B.** LN and GLK-33 bound to human CD33-Fc and CD33 with comparable affinities. **C.-I.** Cytotoxicity assays. *y-axis* shows the relative viability of target cells (% of control). *LV*, lintuzumab vedotin; *GO*, gemtuzumab ozogamicin; *Isotype ADC*, palivizumab-mavg-MMAU DAR8. **J.** Antibody-

dependent cellular cytotoxicity (ADCC) assay. *y-axis* shows the specific lysis of target cells (% of control). **K.** Complement-dependent cytotoxicity (CDC) assay. *y-axis* shows the relative cytotoxicity (% of control). **L.** Cytotoxicity assay of GLK-33 with and without soluble CD33 (sCD33).

Figure 3. *Ex vivo* cytotoxicity assays with patient-derived samples. Cells were incubated with the indicated compounds for five days and IC50 values are presented against **A.** leukemia blasts and **B.** lymphocytes. * = Significant difference according to Kruskal-Wallis test with post-hoc Dunn's test and Bonferroni correction.

Figure 4. *In vivo* evaluation of GLK-33. **A.-D.** HL-60 human leukemia tumor model. Subcutaneously xenografted mice received a single *i.v.* dose of vehicle, LN, or ADC. *Error bars* show the standard error of the mean (SEM). Plotting is stopped when the first animal in the group dies due to disease progression. *LV*, lintuzumab vedotin; *Isotype ADC*, palivizumab-mavg-MMAU DAR8. *Red arrows* show the time of treatment and *black arrows* show the time of the plots in panel **B.** Box and scatter plots of individual tumor volumes at the latest common time point of the groups. Filled box shows the interquartile range (IQR) between the 25th percentile (Q1) and the 75th percentile (Q3). Whiskers show the minimum (Q1 – 1.5 × IQR) and the maximum (Q3 + 1.5 × IQR). Solid line inside the box shows the median and dashed line shows the mean. * = significant difference ($p<0.05$) compared to vehicle according to Kruskal-Wallis test with post-hoc Dunn's test and Bonferroni correction. **C.** Kaplan-Meier plot of progression-free survival (time after treatment until restart of tumor growth) in the middle/low dose groups. **D.** Total human antibody (TAb) and total ADC concentrations in mouse serum. **E.-F.** MOLM-13 human leukemia tumor model. For explanations see panels A.-C.

Figure 5. *In vitro* assays of ADC metabolism with liver microsome preparates from four mammalian species. **A.** Structure of GLK-33 linker-payload and the major metabolic pathways in liver microsome preparates. **B.** Summary of MALDI-TOF mass spectrometric analysis of the ADC degradation

reactions. *Fragment codes* refer to panel A. * P1 and P2 fragments were analyzed as $[M+Na]^+$ ions. **Cys-mavg-MMAE has previously been detected in both rat and human lysosomal preparate metabolism studies (Goldberg *et al.* submitted).

Figure 6. Tolerability and toxicokinetics of GLK-33 in rats. **A.** Overview of study design and observed toxicities. * GLK-33 batch used in the rat study had 10% heavy chain overconjugation (Supplementary Figure 5). **B.** Plasma concentrations of total antibody, ADC based on antibody-conjugated MMAU, and free MMAE at the 20 mg/kg GLK-33 dose level. MMAU concentrations were below the quantitation limit. *Error bars* show the standard deviation. **C.** Toxicokinetic parameters at 10, 20, and 30 mg/kg GLK-33 dose levels. **D.** *In vivo* stability of GLK-33. Human antibody was affinity-isolated from rat plasma on time points up to 9 days after dosing of 30 mg/kg GLK-33 and analyzed by MALDI-TOF mass spectrometry. No signs of linker-payload degradation were observed.

Figure 1.

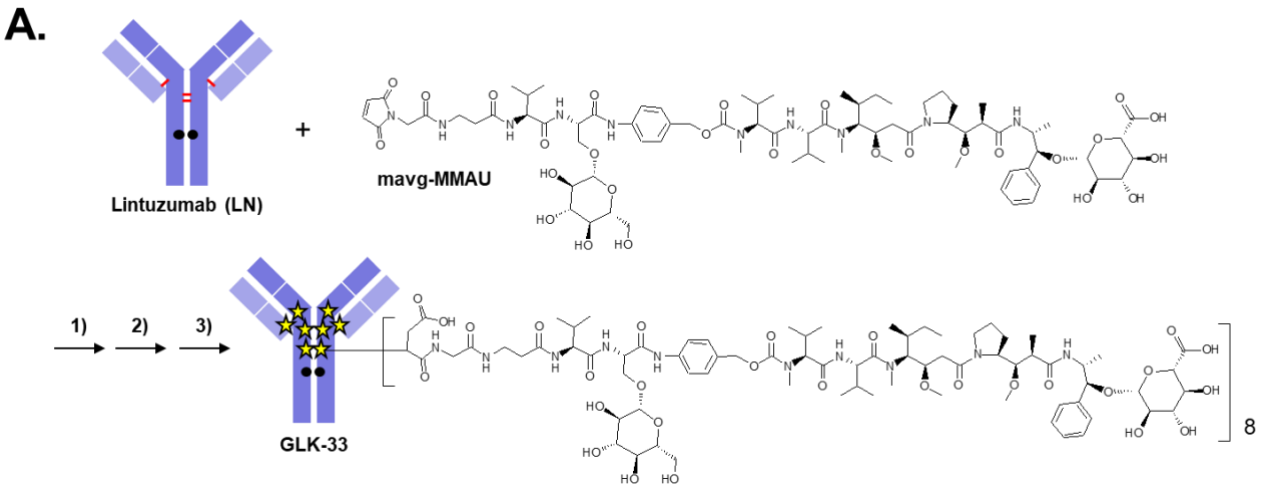
A.
Lintuzumab (LN)
+
mavg-MMAU
1)
2)
3)
GLK-33
8

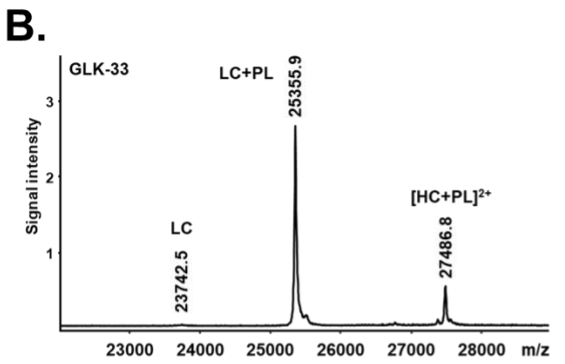
B.
GLK-33
LC+PL
25355.9
[HC+PL]2+
LC
23742.5
27486.8
Signal intensity
m/z

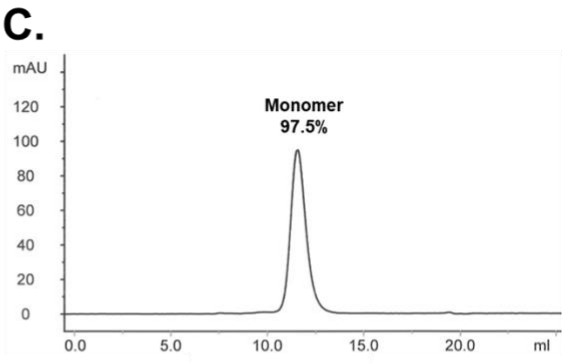
C.
mAU
Monomer
97.5%
ml

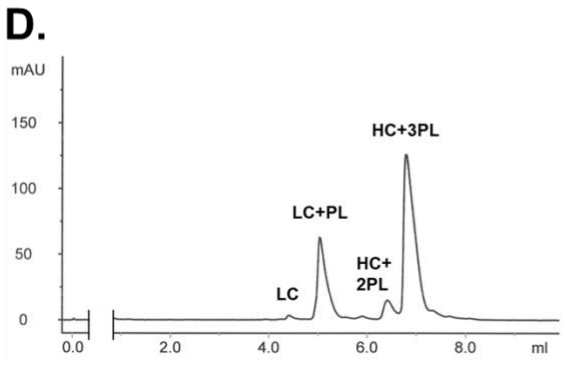
D.
mAU
HC+3PL
LC+PL
HC+
2PL
LC
ml

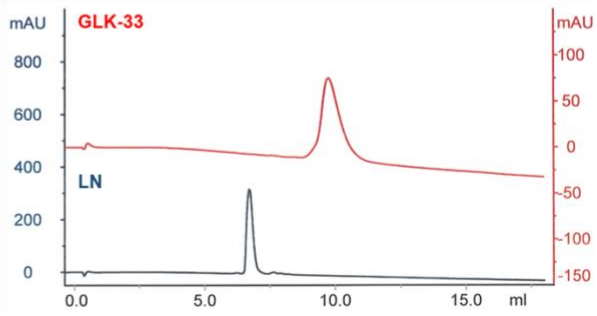
E.
mAU
GLK-33
LN
mAU
ml

Figure 2.

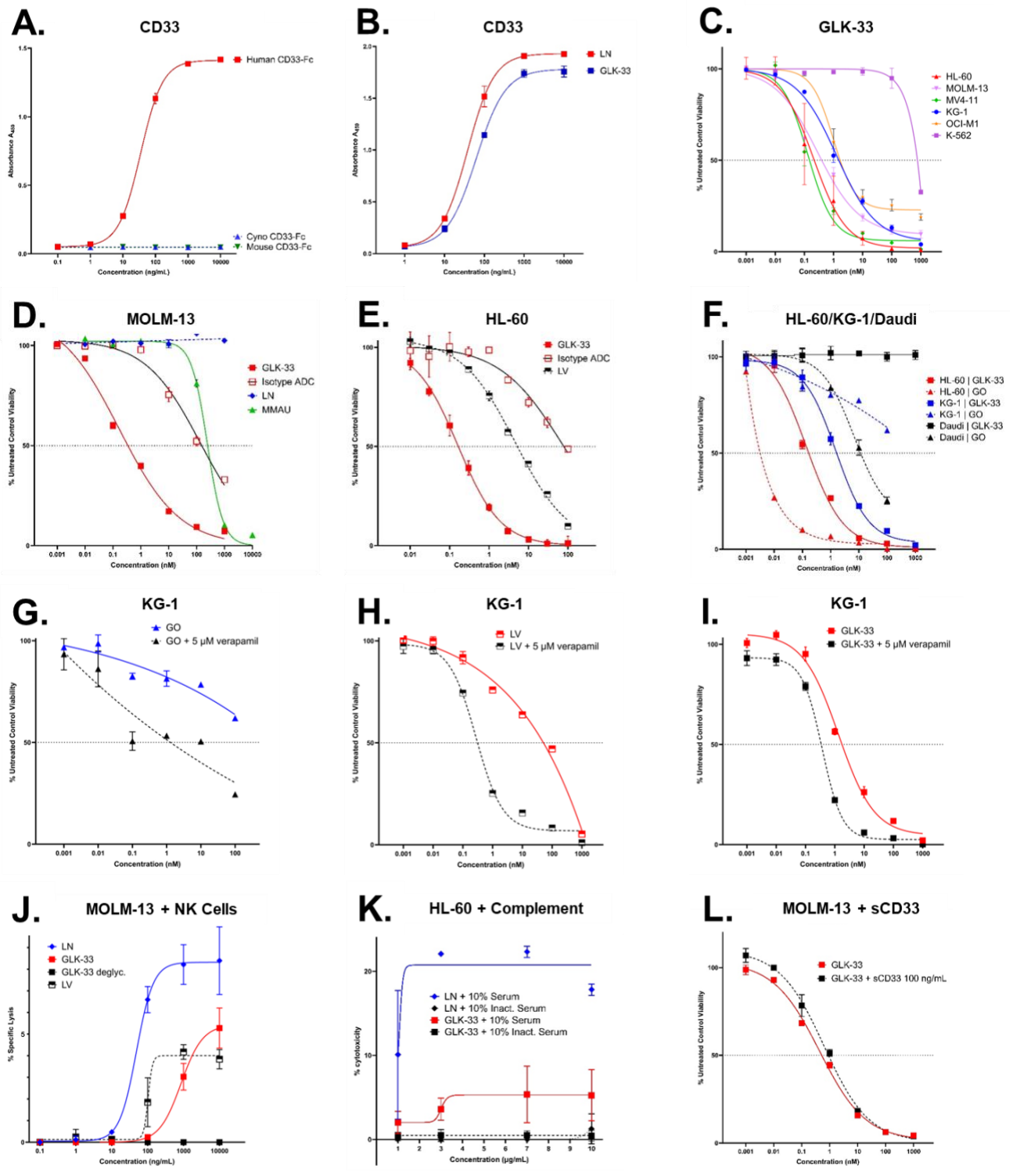
A.
CD33
Human CD33-Fc
Cyno CD33-Fc
Mouse CD33-Fc
Absorbance A450
Concentration (ng/mL)
B.
CD33
LN
GLK-33
Absorbance A450
Concentration (ng/mL)
C.
GLK-33
HL-60
MOLM-13
MV4-11
KG-1
OCI-M1
K-562
% Untreated Control Viability
Concentration (nM)
D.
MOLM-13
GLK-33
Isotype ADC
LN
MMAU
% Untreated Control Viability
Concentration (nM)
E.
HL-60
GLK-33
Isotype ADC
LV
% Untreated Control Viability
Concentration (nM)
F.
HL-60/KG-1/Daudi
HL-60 | GLK-33
HL-60 | GO
KG-1 | GLK-33
KG-1 | GO
Daudi | GLK-33
Daudi | GO
% Untreated Control Viability
Concentration (nM)
G.
KG-1
GO
GO + 5 µM verapamil
% Untreated Control Viability
Concentration (nM)
H.
KG-1
LV
LV + 5 µM verapamil
% Untreated Control Viability
Concentration (nM)
I.
KG-1
GLK-33
GLK-33 + 5 µM verapamil
% Untreated Control Viability
Concentration (nM)
J.
MOLM-13 + NK Cells
LN
GLK-33
GLK-33 deglyc.
LV
% Specific Lysis
Concentration (ng/mL)
K.
HL-60 + Complement
LN + 10% Serum
LN + 10% Inact. Serum
GLK-33 + 10% Serum
GLK-33 + 10% Inact. Serum
% cytotoxicity
Concentration (µg/mL)
L.
MOLM-13 + sCD33
GLK-33
GLK-33 + sCD33 100 ng/mL
% Untreated Control Viability
Concentration (nM)

Figure 3.

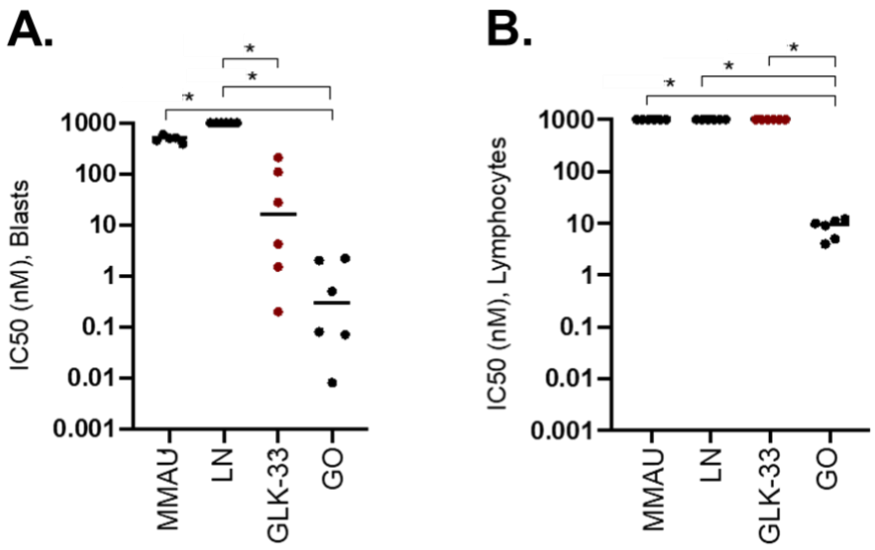
A.
B.
IC50 (nM), Blasts
IC50 (nM), Lymphocytes
1000
100
10
1
0.1
0.01
0.001
MMAU
LN
GLK-33
GO
*

Figure 4.

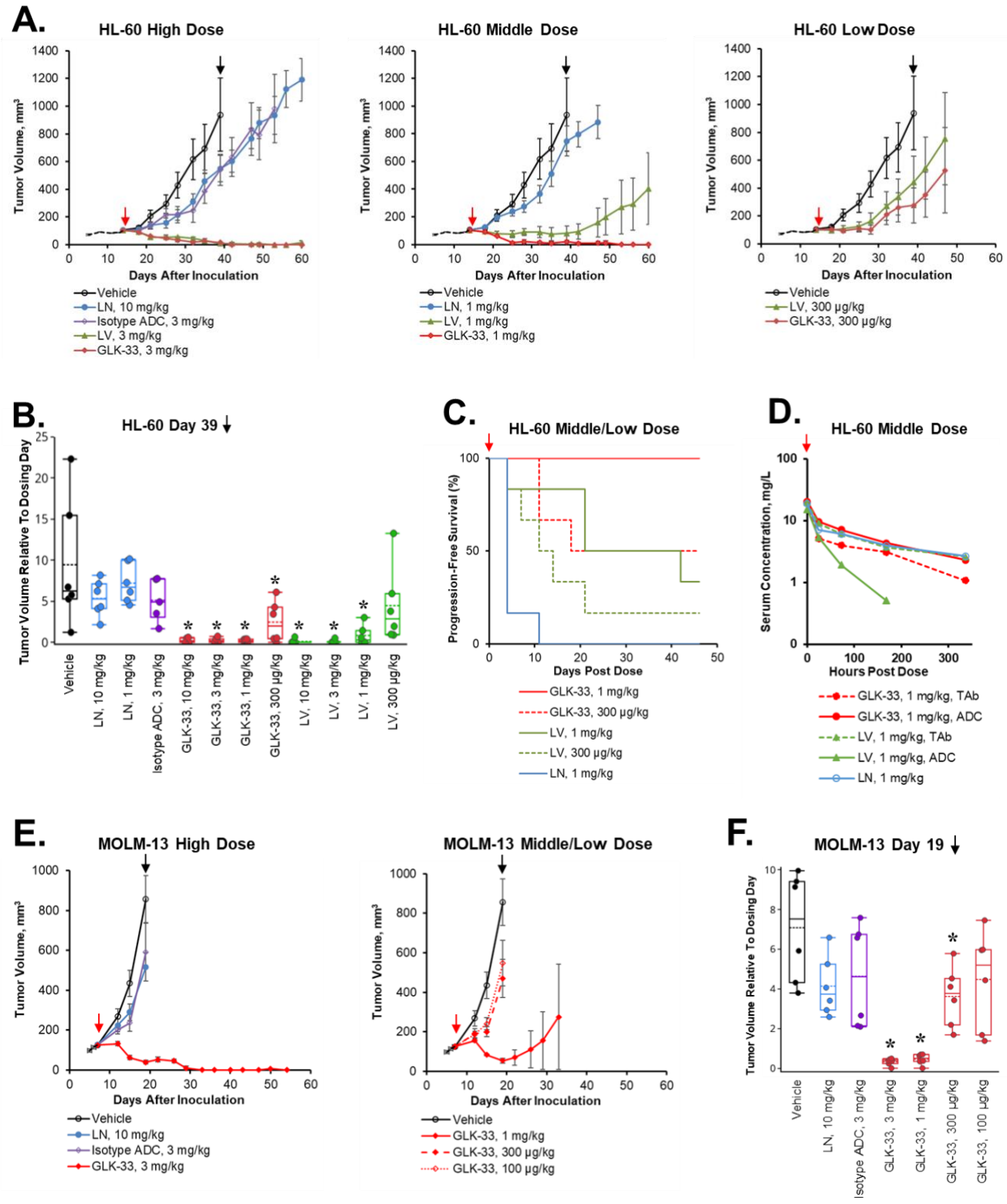
A.
HL-60 High Dose
Tumor Volume, mm³
Days After Inoculation
Vehicle
LN, 10 mg/kg
Isotype ADC, 3 mg/kg
LV, 3 mg/kg
GLK-33, 3 mg/kg
HL-60 Middle Dose
LN, 1 mg/kg
LV, 1 mg/kg
GLK-33, 1 mg/kg
HL-60 Low Dose
LV, 300 µg/kg
GLK-33, 300 µg/kg
B.
HL-60 Day 39
Tumor Volume Relative To Dosing Day
Vehicle
LN, 10 mg/kg
LN, 1 mg/kg
Isotype ADC, 3 mg/kg
GLK-33, 10 mg/kg
GLK-33, 3 mg/kg
GLK-33, 1 mg/kg
GLK-33, 300 µg/kg
LV, 10 mg/kg
LV, 3 mg/kg
LV, 1 mg/kg
LV, 300 µg/kg
C.
HL-60 Middle/Low Dose
Progression-Free Survival (%)
Days Post Dose
GLK-33, 1 mg/kg
GLK-33, 300 µg/kg
LV, 1 mg/kg
LV, 300 µg/kg
LN, 1 mg/kg
D.
HL-60 Middle Dose
Serum Concentration, mg/L
Hours Post Dose
GLK-33, 1 mg/kg, TAb
GLK-33, 1 mg/kg, ADC
LV, 1 mg/kg, TAb
LV, 1 mg/kg, ADC
LN, 1 mg/kg
E.
MOLM-13 High Dose
Tumor Volume, mm³
Days After Inoculation
Vehicle
LN, 10 mg/kg
Isotype ADC, 3 mg/kg
GLK-33, 3 mg/kg
MOLM-13 Middle/Low Dose
GLK-33, 1 mg/kg
GLK-33, 300 µg/kg
GLK-33, 100 µg/kg
F.
MOLM-13 Day 19
Tumor Volume Relative To Dosing Day
Vehicle
LN, 10 mg/kg
Isotype ADC, 3 mg/kg
GLK-33, 3 mg/kg
GLK-33, 1 mg/kg
GLK-33, 300 µg/kg
GLK-33, 100 µg/kg

Figure 5.

A.

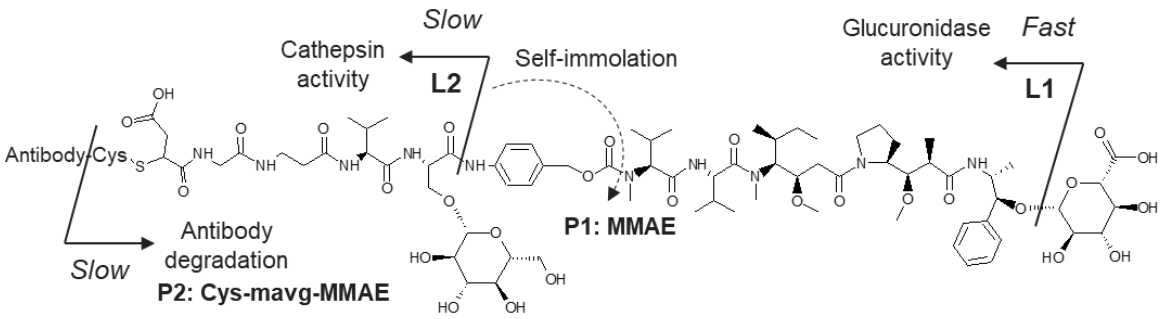

B.

Detected GLK-33 fragments in liver microsome assay

Fragment	m/z	Proposed structure	Rat	Human	Monkey	Pig
L1	-176	Loss of GlcA	+	+	+	+
L2	-1025	Loss of PAB-MMAU	+	+	+	+
P1	740*	MMAE	+	+	+	+
P2	1567*	Cys-mavg-MMAE**	+			

Figure 6.

A.

Toxicology findings	
Test items and dosing	GLK-33*, single *i.v.* bolus
Groups	2 female and 2 male Sprague-Dawley rats/group (n=4), dose levels 10, 20, 30 and 40 mg/kg
Tolerability	10 mg/kg and 20 mg/kg doses were well tolerated 30 mg/kg: 2 females (2/4) euthanized due to symptoms of toxicity and weight loss 40 mg/kg: all animals (4/4) euthanized due to symptoms of toxicity and weight loss
Hematology	≥30 mg/kg: decrease in white blood cells and platelets 40 mg/kg: decrease in red blood cells and hemoglobin
Clinical chemistry	≥30 mg/kg: increase in alanine aminotransferase and amylase 40 mg/kg: decrease in albumin, increase in globulin
Organ weights	≥30 mg/kg: lowered thymus weight
Necropsy findings	≥30 mg/kg: small hematomas in subcutaneous tissue 40 mg/kg: skin ulcers, soft tissue icterus

B.

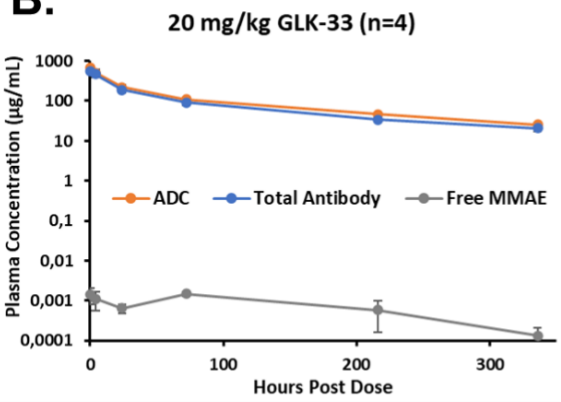

C.

Toxicokinetic parameters	10 mg/kg n=4	20 mg/kg n=4	30 mg/kg n=2
Total antibody			
C_{max} (µg/mL)	301	541	917
AUC_{inf} (µg·d/mL)	752	1300	2266
T½ (d)	3.7	5.1	6.7
ADC			
C_{max} (µg/mL)		665	
AUC_{inf} (µg·d/mL)		1577	
T½ (d)		5.3	
Free MMAE			
C_{max} (ng/mL)		1.5	
AUC_{inf} (ng·d/mL)		11.6	

D.